Scientific Research Publishing

Engineering, 2018, 10, 21-34
http://www.scirp.org/journal/eng
ISSN Online: 1947-394X
ISSN Print: 1947-3931

Enhancing the Creep Resistance of Sn-9.0Zn-0.5Al Lead-Free Solder Alloy by Small Additions of Sb Element

E. A. Eid[1], Manal A. Ramadan[2], A. B. El Basaty[3]

[1]Basic Science Department, Higher Technological Institute, Ramadan, Egypt
[2]Mechanical Engineering Department, Higher Technological Institute, Ramadan, Egypt
[3]Basic Science Department, Faculty of Industrial Education, Helwan University, Cairo, Egypt
Email: ahmedelbasaty@techedu.helwan.edu.eg

How to cite this paper: Eid, E.A., Ramadan, M.A. and El Basaty, A.B. (2018) Enhancing the Creep Resistance of Sn-9.0Zn-0.5Al Lead-Free Solder Alloy by Small Additions of Sb Element. *Engineering*, **10**, 21-34.
https://doi.org/10.4236/eng.2018.101003

Received: December 23, 2017
Accepted: January 28, 2018
Published: January 31, 2018

Copyright © 2018 by authors and Scientific Research Publishing Inc.
This work is licensed under the Creative Commons Attribution International License (CC BY 4.0).
http://creativecommons.org/licenses/by/4.0/

Open Access

Abstract

The creep phenomenon is considered as one of the most important deformation mechanisms under working conditions. The present study has examined the microstructure and creep properties of Sn-9.0Zn-0.5Al solder alloy after adding a small amount of Antimony (Sb). Nominal compositions of Sb additions were chosen to be 0, 0.5, 1.0, and 1.5 wt.%. The minimum strain rate was reduced for the Sb containing solder alloy. The stress exponents, n, were found to be around 3.7 for all soldiers at 130˚C. The stress exponent increases as the temperature drops from 100˚C to 50˚C, except for the 1.0% Sb alloy, where n 5.3 - 6.1 at all the temperature range (T = 50˚C, 100˚C and 130˚C). The results reveal that the Sb-containing solder alloys have better creep resistance with greater ductility than the Sb-free alloy due to solid solution strengthening, and intermetallic compound SnSb particle hardening.

Keywords

Sn-Zn-Al-Sb Alloys, Lead Free Solders, Sb Addition, Creep Properties

1. Introduction

Sn-9Zn eutectic alloy has been considered as one of the candidate that can be replaced the Sn-37Pb solder without increase of the operating temperature. Apart from its favorable melting temperature of solder alloys, Sn-9Zn alloy has better mechanical properties than the conventional Sn-Pb solders [1] [2] [3], and a lower cost than other Lead-free solders alloys [4] [5]. Whenever such alloys are used for many electronic applications, they are subjected to yield many prob-

lems, such as, the tendency of oxidation and poor wetting ability [5]. Therefore, the researchers tried to add a third element to overcome the shortfalls of Sn-9Zn alloy. Consequently, it is necessary to understand how the oxidation resistance, wettability, corrosion, melting temperature, and mechanical properties are changed because of the third alloying element addition.

For example, the third element suggesting adding to Sn-9Zn eutectic alloy are Ag [4] [5], Bi [6] [7], In [8], Al [9] [10] and Ce/La [11] [12]. For instance, McCormack and Jin [8] found that small additions of 5% In can improve the ductility of Sn-Zn base solders. It was found also that the wetting characteristics are improved when Ag is added [5] [13]. Moreover, Kim *et al*. [6] found that with increasing of additional Bi content, the melting temperature decreased from 198.4˚C to 186.1˚C. However, the alloys with a high Bi content need to be controlled because of the brittle nature of Bi and the strong tendency for segregation [6] [14]. Chen and Li [15] reported that adding 1.0 wt.% Sb into Sn-Ag-Cu solder alloy could lower the activity of Sn by forming SnSb compound. They proposed that SnSb particle might be initially formed and finally dispersed in the molten solder to increase the nucleation rate and refine the grain size. It is further found in tensile tests that mechanical properties are improved when the solder matrix is evenly dispersed with intermetallic compound (IMC) and SbSn particles [15] [16] [17] [18] [19].

Recently, our group reveled that adding a small amount of Sb to the Sn-9Zn-0.5Al system refined the bulky needles of Zn as well as β-Sn matrix. In addition, it improved strengthen by solid solution hardening mechanism [3]. In same time, it is known that under the conventional operating conditions, the solder joints are exposed to aggressive thermo-mechanical cycling (TMC), with imposed shear strain under high homologous temperatures T_H ($T_H = T/T_m$) [20]. Therefore, the creep phenomenon is considered as the most important deformation mechanism under working conditions. Additionally, the literatures have rare studies about the effect of Sb as an alloying element on the creep properties of Sn-Zn-Al solder system. Therefore, the present study focused on the effect of Sb alloying element on the reliability characteristics of Sn-9.0Zn-0.5Al solder alloy based on microstructural, and creep tensile properties. We have chosen small percentages of the Sb added to Sn-Zn-Al solder alloy to make a solid solution of Sb within Sn matrix, which enhanced the creep resistance and rapture time of our solder alloy [1] [3]. Within this scope, the creep tests were performed under constant applied stresses ranging from 15.6 to 29.3 MPa at constant temperatures of 50˚C, 100˚C, and 130˚C.

2. Experimental Work

Table 1 shows the chemical compositions of solders used in this study. Each solder was made with pure Sn, Zn, Al and Sb (purity 99.99%). The constituent elements were melted in vacuum Pyrex tube and maintained at 150˚C above their respective melting point for 20 minutes, then cast into steel mold, and

Table 1. Compositions of the solder alloy (wt. %).

Alloy	abbreviation	Sn	Zn	Al	Sb
Sn-9.0Zn-0.5Al	SZA905	Bal.	9.02	0.51	0.00
Sn-9.0Zn-0.5Al-0.5Sb	SZA-0.5Sb	Bal.	9.01	0.50	0.51
Sn-9.0Zn-0.5Al-1.0Sb	SZA-1.0Sb	Bal.	9.02	0.52	1.03
Sn-9.0Zn-0.5Al-1.5Sb	SZA-1.5Sb	Bal.	9.02	0.52	1.52

air-cooled to the room temperature. The air-cooling is equivalent to that adopted in the particle reflow process in industry. The cooling rate estimated by using a thermocouple placed in the center of solder. The ingots were cold drawn to wire samples of 8×10^{-4} m in diameter and 5×10^{-2} m length. To obtain stabilized microstructures, the alloy samples were aged at 130˚C for 3 hours, and then slow cooled to room temperature. The as-solidified microstructure of the solders was investigated using X-ray diffraction (Philips Analytical X-Ray PW3710) and Nikon optical microscope, where the grain sizes was estimated using a linear intercept technique. Tensile creep tests were performed using homemade instrument, the resulting strain recorded as a function of time under constant applied stresses ranging from 15.6 to 29.3 MPa at constant temperatures of 50˚C, 100˚C, and 130˚C. The accuracy of temperature measurement is of the order 1˚C. Strain measurements were done with an accuracy of 1×10^{-2} mm.

3. Results and Discussion

3.1. As-Solidified Microstructure

Optical micrographs of specimens with varying x % Sb (x = 0, 0.5, 1.0 and 1.5) contents are presented in **Figure 1**. The bright-gray area and dark-gray area in **Figure 1** denotes the primary β-Sn phase and eutectic (Sn + Zn) networks, respectively. This result is consistent with binary-phase diagram of Sn-Zn, which shows a typical binary-eutectic phase diagram with no intermetallic compounds and limited solubility of the two elements in each phase [9]. Much coarser primary β-Sn grains can be found only in the Sn-9.0Zn-0.5Al (SZA905) alloy as shown in **Figure 1(a)**. In addition, the microstructure of the Sb-free alloy is not uniform. The formation of fully individualized and spheroid grains occurred during solidification at cooling rate of 10˚C/s. Similar microstructures are observed in some Lead-free solder alloys at earlier solidification rates of 12˚C/s and 10˚C/s in studies [17]. **Figures 1(b)-(d)** show that the originally coarse β-Sn grains were refined which is due to the amount of Sb-addition in the Sn-9.0Zn-0.5%Al alloy. The addition of Sb promotes the formation of an equated array of grains with a wavy or curved phase boundaries. **Figure 1(c)** also reveals that the reduction in the grain size is most effective as Sb content up to 1.0%. Therefore, it is assumed from the microstructure that the amount of Sb dissolved in Sn rich phase varies depending on the Sn-9.0Zn-0.5Al-xSb solder composition. According to phase diagram analysis and work done by other

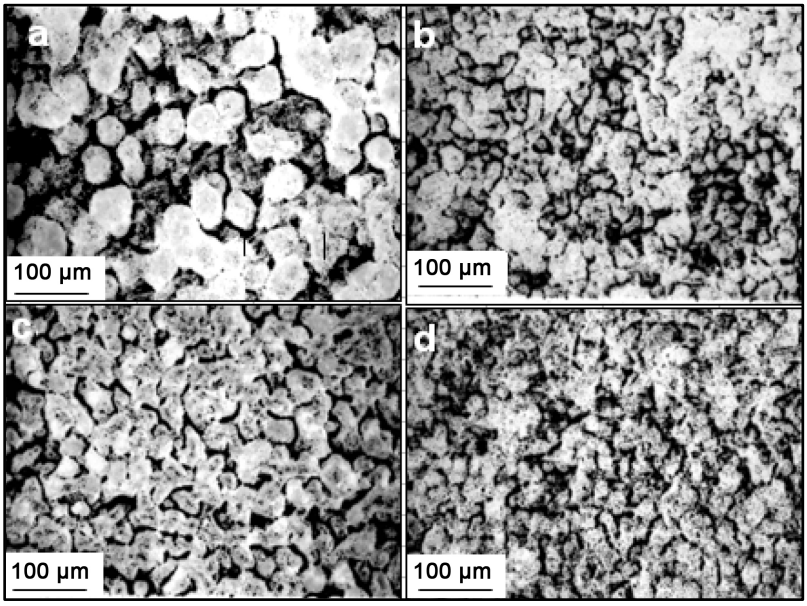

Figure 1. Optical images of the four solder alloys microstructure after annealing at 13˚C for 3 h of composition (a) Sn-9.0Zn-0.5Al, (b) Sn-9.0Zn-0.5Al-0.5Sb, (c) Sn-9.0Zn-0.5Al-1.0Sb, and (d) Sn-9.0Zn-0.5Al-1.5Sb.

authors [2] [18] [21] [22] [23] [24], at a temperature above 234.8˚C, the presence of Sb in Sn-Zn eutectic seems to simulate the formation of SnSb intermetallic compound (IMC) in molten solder. The SnSb phase is a stable phase and exists in the form of small particles that are finally dispersed in the matrix phase [23], which offers preferred sites for nucleation, resulting in grain refining and uniform microstructure as reported in our previous work [3].

The XRD micrographs for Sn-9.0Zn-0.5Al-x Sb% (x = 0.0, 0.5, 1.0 and 1.5 wt %) lead free solder alloys are depicted in **Figure 2**. Presence of (200), (101), (211) and (321) peaks at 2θ values of 31.2˚, 33.6˚, 45.3˚, and 64.8˚ respectively, confirm the formation of body centered tetragonal (BCT) crystal structure of β-Sn for all investigated alloys. Meanwhile, the XRD patterns of Sb-containing alloys exhibited obviously decrement in intensity of (002) and (100) of Zn crystallographic textures. The latter observation is detail discussed in our pervious article, which confirmed hypoeutectic composition is formed [3]. On other hand, no peaks of Al element were observed while SbSn IMC phase was detected as a small peak for 1.5 wt % Sb-content solder. That indicated the Sb atoms have successfully replaced the corresponding position of Sn atoms at BCT lattice sites for SZA-1.5 Sb lead free solder alloys [24].

3.2. Features of Creep Behavior

Figures 3(a)-(c) show the results of creep test obtained for Sn-9.0Zn-0.5Al-xSb (x = 0.0%, 0.5%, 1.0%, and 1.5%) solder alloys. The samples were investigated at temperatures of 50˚C, 100˚C, and 130˚C under different constant stresses (15.6 - 29.3 MPa). The trend in the creep curves at all levels of applied stresses and temperatures suggests a rapid transition from a little primary creep regime, to an extended period of constant strain rate with tertiary creep regime. This transition

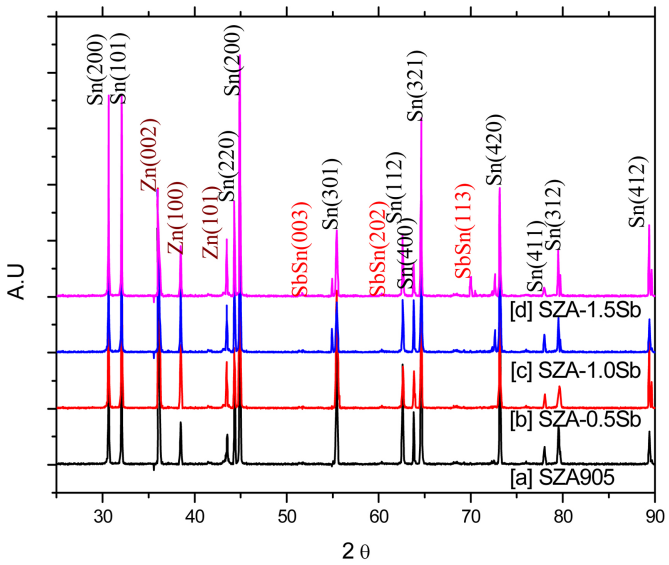

Figure 2. XRD patterns for as-solidified solder alloys (a) Sn-9.0Zn-0.5Al, (b) Sn-9.0Zn-0.5Al-0.5Sb, (c) Sn-9.0Zn-0.5Al-1.0Sb and (d) Sn-9.0Zn-0.5Al-1.5Sb.

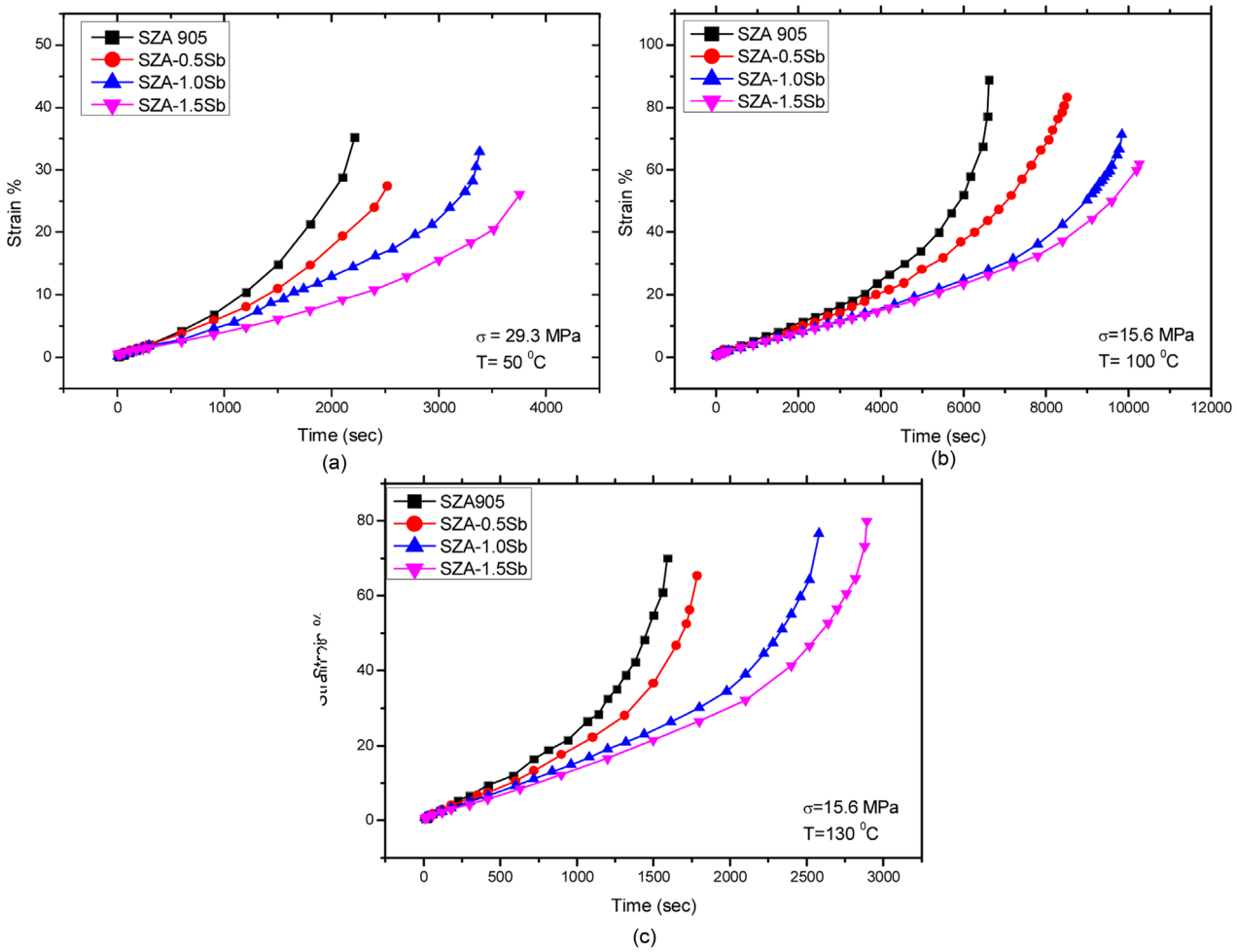

Figure 3. Comparison of the creep behavior of the four solder alloys under different stress at (a) 50˚C, (b) 100˚C and (c) 130˚C.

is easier to observe in the plot of strain rate versus time that is presented in Figure 4(a) and Figure 4(b). The materials showed characteristics of secondary and tertiary creep after loading with very little primary creep. Since the stress and temperature are constants, the variation in creep strain rate suggests a basic change in the internal structure of the alloy during time. The strain hardening in the primary creep was rapidly recovered and balanced in the steady state stage. However, effects of Sb addition on the creep curves are also presented in Figures 3-5. Additions of Sb not only reduced the strain rate but also increased the rapture

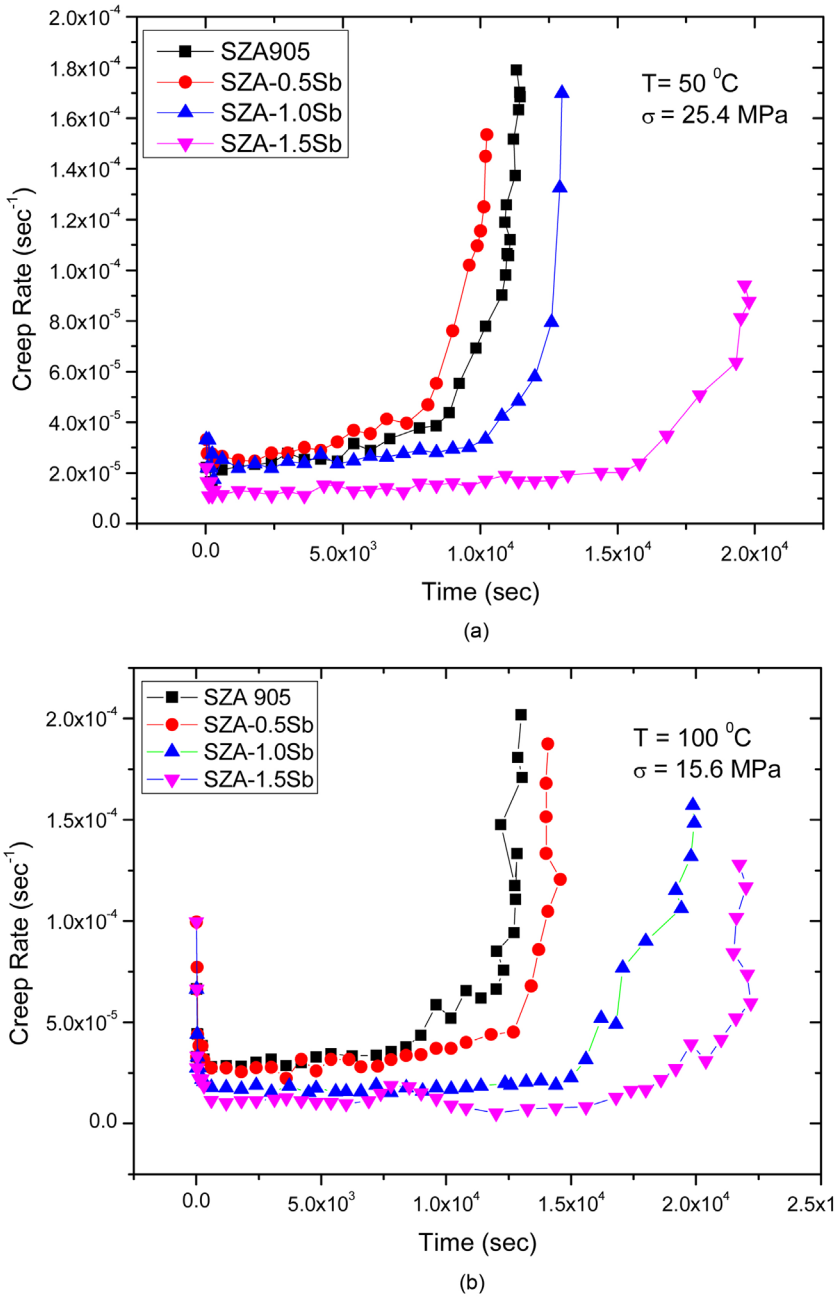

Figure 4. Creep rate-time curve of the Sn-9.0Zn-0.5Al-x Sb% lead free solder alloys at (a) T = 50˚C and (b) T = 100˚C.

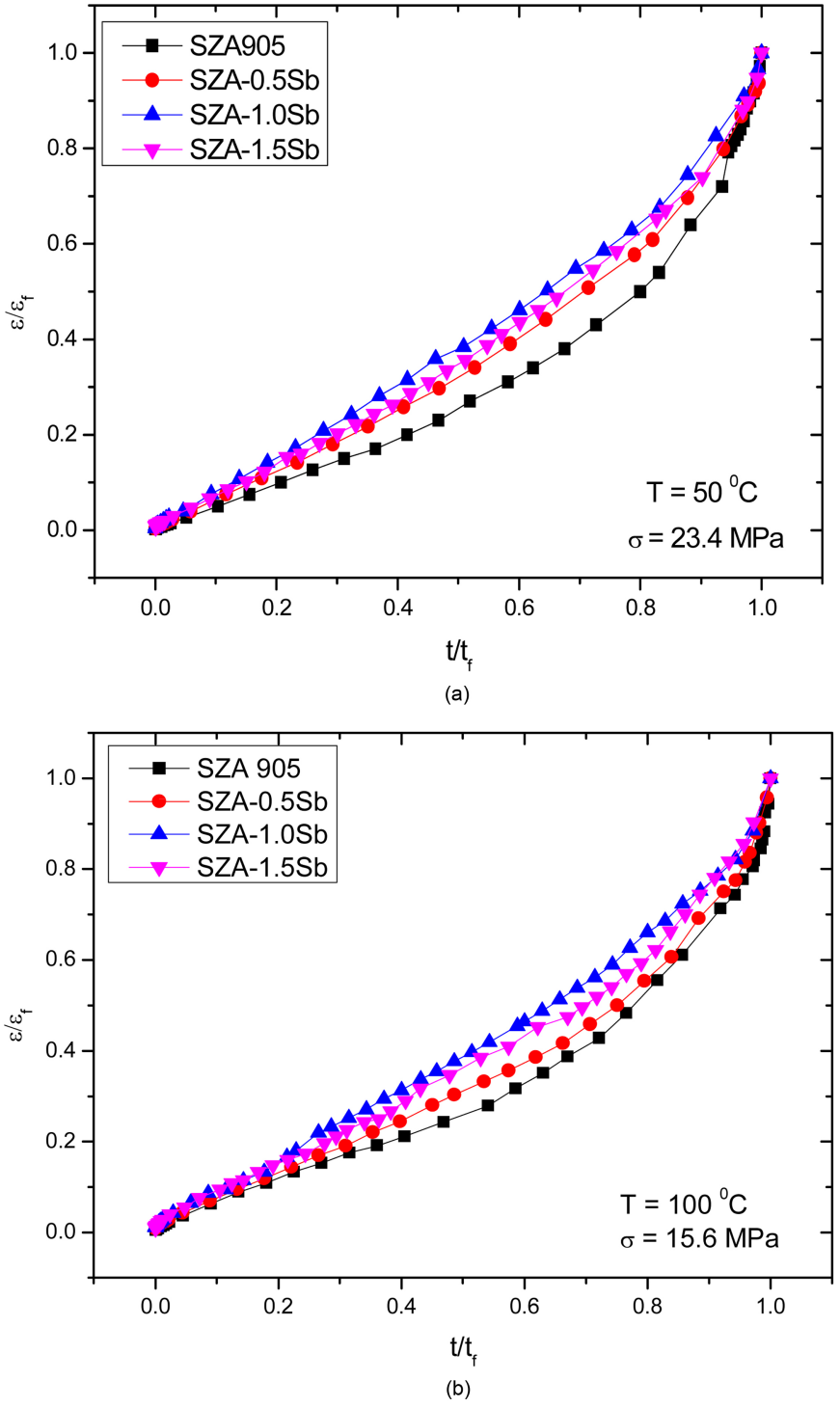

Figure 5. Normalized creep curve of Sn-9.0Zn-0.5Al-x Sb% at (a) T = 50˚C and (b) T = 100˚C.

time, and the significant effect was at Sb content 1.0%.

The specific features of the creep for the four alloys at temperatures of 50 and 100˚C are compared in **Figure 5(a)** and **Figure 5(b)**, in which creep strain (ε) and time (t) are normalized with respect to the rupture strain (ε_f) and rupture

time (τ_f), respectively. At 50˚C, the fraction of the steady-state creep strain increased against the rupture strain ($\varepsilon_s/\varepsilon_f$) because of Sb additions, and that effect was maximized at 1.0% Sb. Whereas increasing the temperature from 50˚C to 100˚C resulted in decreasing the fraction ($\varepsilon_s/\varepsilon_f$) for the 1.0% Sb alloy and enhanced the creep resistance (*i.e.*, lowered) which is associated with the dissolution of Sb rich β-Sn phase in the matrix [25].

3.3. Stress Dependence of Minimum Creep Rate

The minimum strain rate was measured as a function of stress and temperature from the linear portions of the creep curves for the four solder compositions. Stress exponents, n, were calculated from the power-law creep expression, $\dot{\varepsilon}_{\min} \sim \sigma_n$, where $\dot{\varepsilon}_{\min}$ is the minimum creep rate and σ is the applied stress. Log-Log plots of the minimum strain rate as a function of stress for the four solder alloys are given in **Figures 6(a)-(d)**. The calculated values of n from the data in **Figure 6** are plotted versus temperature in **Figure 7**. The 1.0% Sb alloy showed the best

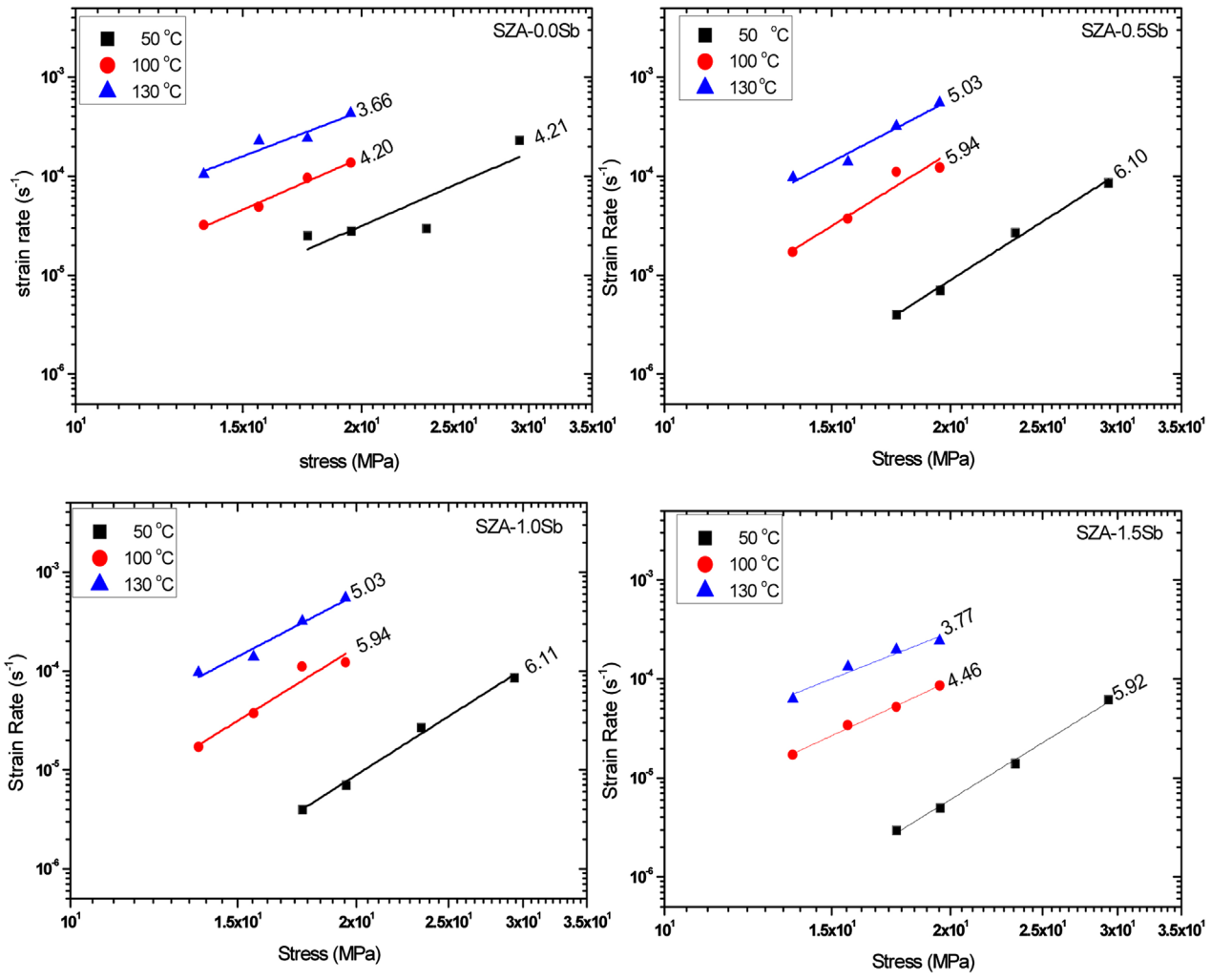

Figure 6. Steady-state creep rate $\dot{\varepsilon}$, plotted against applied stresses, σ, at various temperatures, T, in double logarithmic scales of the four solder alloys.

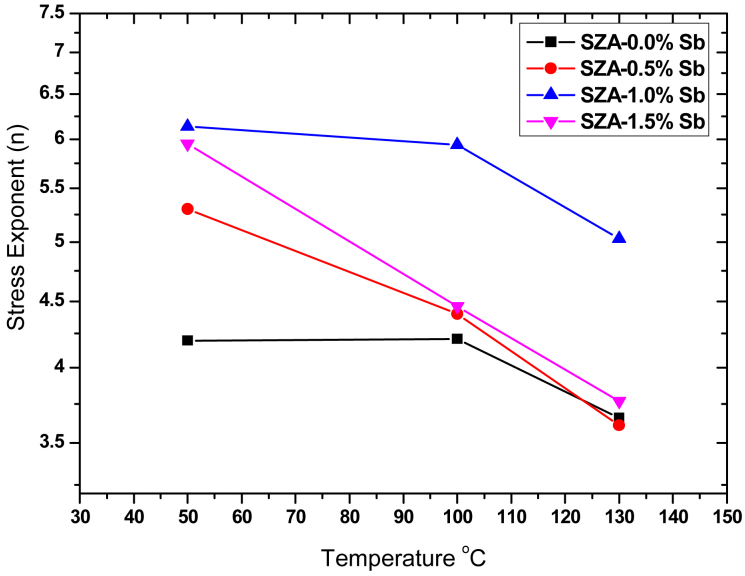

Figure 7. Stress exponent, n, dependence of temperature for investigated solders alloys.

creep resistance at all the temperature range, while the Sb-free alloy showed the worst one. The major anomaly in the data is in the temperature dependence of stress exponent. At 130˚C, n values were usually around 3.7 for all solder alloys except for 1.0% Sb specimens, which showed high n value of 5.3. The values of stress exponents for all solder alloys increase rapidly as the temperature decreases from 100˚C to 50˚C, except the 1.0% Sb alloy which showed almost identical stress exponent of 5.3 - 6.1 at 50˚C and 100˚C, a range of significant technological interest.

It appears that the amount of Sb dissolved in the solution-strengthened matrix phase varies with different Sn-9.0Zn-0.5Al solder systems. It is assumed that the stable characteristics of mechanical properties resulted in the strengthening effect of the solute concentration [2] [18] [22]. Sb element has higher affinity to the constituent element of Sn in the Sn-Zn-Al-Sb quaternary system. It will reduce the activity of Sn by forming solid solution hardening and particle hardening of Sb rich β-Sn phase, resulting in refinement of the grain size, and thus improved the creep resistance as reported by Chen *et al.* [15]. However, the change in creep behavior with temperature is consistent with the observations of Song and Morris [21], Breen and Weertman [26], Suh *et al.* [27], and Poirie [28]. They noted significant changes in creep behavior of Sn-rich solders at about 100˚C. The data presented in **Figure 7** show the range of stress exponent (n ~ 3.7 - 6.1) is comparable to that of Sn and Sn-rich solders, corresponding to climb-controlled creep (n~4 - 5) reported by Breen and Weertman [26] and Song and Morris [21]. Dislocation climb-controlled creep is generally described by a power law equation of the form [22] [31]:

$$\dot{\varepsilon} = A(\sigma)^n \exp(-Q/RT) \tag{1}$$

where A is a constant, R is the gas constant, n is the stress exponent and Q is the

activation energy. The apparent activation energy, *Q*, of the creep process was determined from Arrhenius plot ($\log \dot{\varepsilon}$ versus 1/T), as shown in Figure 8, the values of, *Q*, for the process estimated to be 40 ± 2 kJ/mole for Sb-containing solders and Sb-free solder alloy as depicted in Figure 9, which are comparable to that reported for the pipe diffusion controlled climb of tin (43 - 46 kJ/mole) [29]

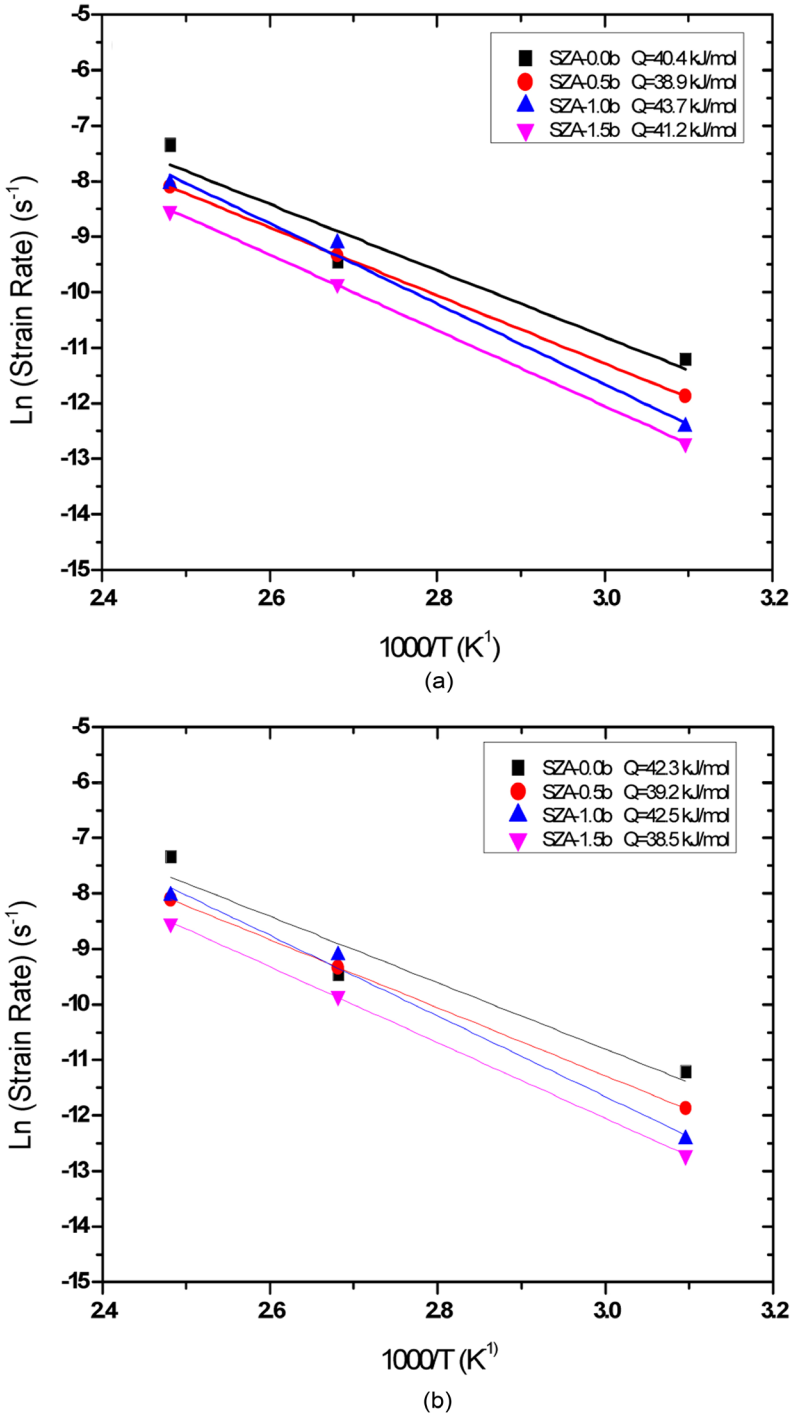

Figure 8. Effect of temperature on the steady–state creep rate of the four solder alloys at: (a) σ= 17.55 MPa, and (b) σ= 19.50 MPa.

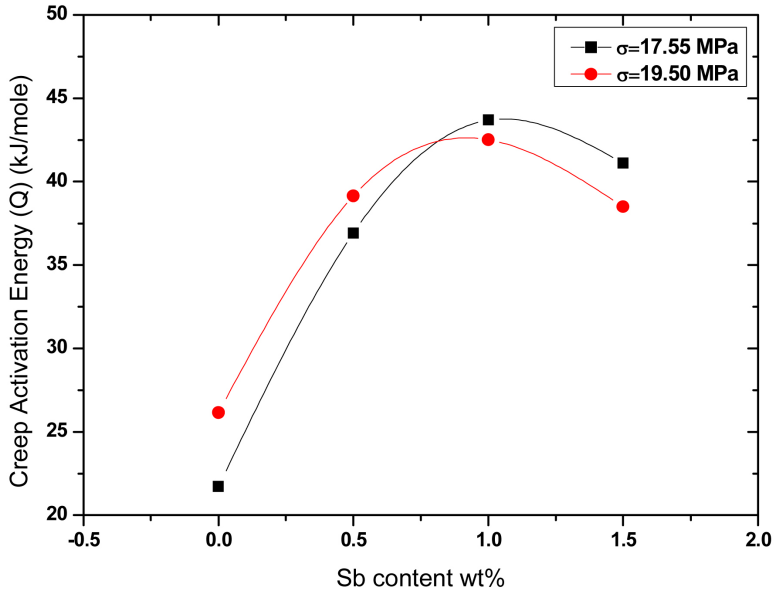

Figure 9. Activation energy dependence on the Sb content in Sn-8.9Zn-0.25Al solder alloys at different applied stress.

[30] [31]. From this analysis, no evidence for different creep mechanisms operating in the high and low temperature range was found. For more confirmation, the observed change in creep rates, $\dot{\varepsilon}_{\min}$, between the Sb-free solder and Sb-containing solders clearly indicates the dominance of climb dislocation mechanism since diffusion creep would not be affected by the grain size in the present alloys. From these finding, one can seen that this low correlation between both the mechanical property data and the activation energies for the ternary Sn-9.0Zn-0.5Al and the quaternary ternary Sn-9.0Zn-0.5Al-xSb solder alloys leads to conclude that the crystallographic texture particularly in as-solidified solder plays an important role for determining the nature of creep deformation. This in turn, implies that the bulk inter-granular processes and dislocation movement are of high importance, particularly in the view of the main difference in the slip behavior of the constituent phases.

4. Conclusions

The main conclusions to be drawn from this study may be summarized as follows:

1) The originally coarse β-Sn grains in the microstructure of Sn-9.0Zn-0.5Al solder alloy were refined and become uniform after Sb additions due to the solute concentration and the finally dispersed SnSb particles in the matrix, which offer preferred sites for nucleation during solidification.

2) The Sb-containing solders have better creep resistance and greater ductility than the Sn-9.0Zn-0.5Al solder alloy, and the effect was usually found to reduce and increase rupture time τ_f.

3) The stress exponents were usually around 3.7 for all solders at 130˚C except

for 1.0 wt.% Sb addition, which showed 5.3, and have a temperature dependence.

4) The activation energies for all compositions were estimated to be 40.2 kJ/mol, confirming pipe diffusion controlled climb of β-Sn.

References

[1] Abtew, M. and Selvaduray, G. (2000) Lead-Free Solders in Microelectronics. *Materials Science and Engineering*, **27**, 95-141. https://doi.org/10.1016/S0927-796X(00)00010-3

[2] Puttlitz, K.J. and Stalter, K.A. (2004) Handbook of Lead-Free Solder Technology for Microelectronic Assemblies. Marcel Dekker, Inc., 292-294.

[3] El Basaty, A.B., Deghady, A.M. and Eid, E.A. (2017) Influence of Small Addition of Antimony (Sb) on Thermal Behavior, Microstructural and Tensile Properties of Sn-9.0Zn-0.5Al Pb-Free Solder Alloy. *Materials Science and Engineering A*, **701**, 245-253. https://doi.org/10.1016/j.msea.2017.06.092

[4] Chang, T.C., Hon, M.H. and Wang, M.C. (2003) Intermetallic Compounds Formation and Interfacial Adhesion Strength of Sn-9Zn-0.5Ag Solder Alloy Hot-Dipped on Cu Substrate. *Journal of Alloys and Compounds*, **352**, 168. https://doi.org/10.1016/S0925-8388(02)01122-2

[5] El-Daly, A.A., Swilem, Y., Makled, M.H., El-Shaarawy, M.G. and Abdraboh, A.M. (2009) Thermal and Mechanical Properties of Sn-Zn-Bi Lead-Free Solder Alloys. *Journal of Alloys and Compounds*, **484**, 134-142. https://doi.org/10.1016/j.jallcom.2009.04.108

[6] Kim, Y.S., Kim, K.S., Hwang, C.W. and Suganuma, K. (2003) Effect of Composition and Cooling Rate on Microstructure and Tensile Properties of Sn-Zn-Bi Alloys. *Journal of Alloys and Compounds*, **352**, 237. https://doi.org/10.1016/S0925-8388(02)01168-4

[7] Hirose, A., Yanagawa, H., Ide, E. and Kobayashi, K.F. (2004) Joint Strength and Interfacial Microstructure between Sn-Ag-Cu and Sn-Zn-Bi Solders and Cu Substrate. *Science and Technology of Advanced Materials*, **5**, 267. https://doi.org/10.1016/j.stam.2003.10.024

[8] McCormack, M. and Jin, S. (1994) New Lead-Free Solders. *Journal of Electronic Materials*, **23**, 635. https://doi.org/10.1007/BF02653349

[9] Lin, K.L., Wen, L.H. and Liu, T.P. (1998) The Microstructures of the Sn-Zn-Al Solder Alloys. *Journal of Electronic Materials*, **27**, 97-105. https://doi.org/10.1007/s11664-998-0197-x

[10] Lin, K.L. and Wang, Y.C. (1998) Wetting Interaction of Pb-Free Sn-Zn-Al Solders on Metal Plated Substrate. *Journal of Electronic Materials*, **27**, 1205. https://doi.org/10.1007/s11664-998-0070-y

[11] Wang, L., Yu, D.Q., Zhao, J. and Huang, M.L. (2002) Improvement of Wettability and Tensile Property in Sn-Ag-RE lead-Free Solder Alloy. *Materials Letters*, **56**, 1039-1042. https://doi.org/10.1016/S0167-577X(02)00672-9

[12] Wu, C.M.L., Yu, D.Q., Law, C.M.T. and Wang, L. (2004) Properties of Lead-Free Solder Alloys with Rare Earth Element Additions. *Materials Science and Engineering: R: Reports*, **44**, 1. https://doi.org/10.1016/j.mser.2004.01.001

[13] McMormack, M. and Jin, S. (1994) Improved Mechanical Properties in New, Pb-Free Solder Alloys. *Journal of Electronic Materials*, **23**, 715. https://doi.org/10.1007/BF02651364

[14] Date, M., Tu, K.N., Shoji, T., Fujiyoshi, M. and Soto, K. (2004) Interfacial Reactions

and Impact Reliability of Sn-Zn Solder Joints on Cu or Electroless Au/Ni(P) Bond-Pads. *Journal of Materials Research*, **19**, 2887. https://doi.org/10.1557/JMR.2004.0371

[15] Chen, B.L. and Li, G.Y. (2005) An Investigation of Effects of Sb on the Intermetallic Formation in Sn-3.5Ag-0.7Cu Solder Joints. *IEEE Transactions on Components and Packaging Technologies*, **28**, 534-541. https://doi.org/10.1109/TCAPT.2005.848573

[16] Beshai, M.H.N., Habib, S.K., Yassein, A.M. and Saad, G. (1999) Effect of SnSb Particle Size on Creep Behaviour under Power Law Regime of Sn-10%Sb Alloy. *Crystal Research and Technology*, **34**, 119. https://doi.org/10.1002/(SICI)1521-4079(199901)34:1<119::AID-CRAT119>3.0.CO;2-1

[17] Shohji, I., Yoshida, T., Takahashi, T. and Hioki, S. (2004) Tensile Properties of Sn-Ag Based Lead-Free Solders and Strain Rate Sensitivity. *Materials Science and Engineering*: *A*, **366**, 50. https://doi.org/10.1016/j.msea.2003.09.057

[18] Chang, T.-C., Hon, M.-H., Wang, M.-C. and Lin, D.-Y. (2004) Effect of Thermal Cycling on the Adhesion Strength of Sn-9Zn-xAg-Cu Interface. *IEEE Transactions on Advanced Packaging*, **27**, 158-164.

[19] Chen, B.L. and Li, G.Y. (2004) Influence of Sb on IMC Growth in Sn-Ag-Cu-Sb Pb-Free Solder Joints in Reflow Process. *Thin Solid Films*, **462**, 395-401. https://doi.org/10.1016/j.tsf.2004.05.063

[20] Sarihan, V. (1993) Temperature Dependent Viscoplastic Simulation of Controlled Collaps under Thermal Cycling. *Journal of Electronic Packaging*, **115**, 16. https://doi.org/10.1115/1.2909295

[21] Song, H.G., Morris Jr., J.W. and Hua, F. (2002) Anomalous Creep in Sn-Rich Solder Joints. *Materials Transactions*, **43**, 1847.

[22] El-Daly, A.A. (2004) Tensile Properties of Pb-Sn Bearing Alloy Containing Small Amount of Sb. *Physica Status Solidi* (*a*), **201**, 2035. https://doi.org/10.1002/pssa.200306813

[23] Hansen, M. (1958) Constitution of Binary Alloys. McGraw-Hill Book INC, New York, 1217.

[24] Chang, T.C., Hon, M.H. and Wang, M.C. (2004) Electrochemical Behaviors of the Sn-9Zn-xAg Lead-Free Solders in a 3.5 wt% NaCl Solution. *Journal of the Electrochemical Society*, **151**, C484-C491. https://doi.org/10.1149/1.1756890

[25] Shin, S.W. and Yu, J. (2003) Creep Deformation of Lead-Free Sn-3.5Ag-Bi Solders. *Japanese Journal of Applied Physics*, **42**, 1368. https://doi.org/10.1143/JJAP.42.1368

[26] Breen, J.E. and Weertman, J. (1955) Creep of Polycrystalline Tin. *JOM*: *Journal of the Minerals, Metals, and Materials Society*, **203**, 1230. https://doi.org/10.1007/BF03379034

[27] Suh, S.H., Cohen, J.B. and Weertman, J. (1983) X-Ray Diffraction Study of Subgrain Misorientation during High Temperature Creep of Tin Single Crystals. *Metallurgical Transactions A*, **14**, 117. https://doi.org/10.1007/BF02643744

[28] Poirier, J.P. (1978) Is Power-Law Creep Diffusion-Controlled? *Acta Metallurgica*, **26**, 629.

[29] Igoshev, V.J. and Kleiman, J.I. (2000) Creep Phenomena in Lead-Free Solders. *Journal of Electronic Materials*, **29**, 244. https://doi.org/10.1007/s11664-000-0150-0

[30] Reinikinen, T. and Kivilahti, J. (1999) Deformation Behavior of Dilute SnBi (0.5 to 6 at. pct) Solid Solutions. *Metallurgical and Materials Transactions A*, **30**, 123. https://doi.org/10.1007/s11661-999-0200-z

[31] Eid, E.A., Fouda, A.N. and Duraia, E.-S.M. (2016) Effect of Adding 0.5 wt% ZnO Nanoparticles, Temperature and Strain Rate on Tensile Properties of Sn-5.0 wt% Sb-0.5 wt% Cu (SSC505) Lead Free Solder Alloy. *Materials Science and Engineering*: *A*, **657**, 104-114. https://doi.org/10.1016/j.msea.2016.01.081